https://doi.org/10.48047/AFJBS.7.8.2025.190-204

African Journal of Biological Sciences

Journal homepage: http://www.afjbs.com

Research Paper Open Access

Chemical profiling, DFT and docking calculations of Petroleum ether extract from Algerian *Suaeda fruticosa* Forssk. Ex J.F.Gmel

Remouche Fairouz[1], Hamza Allal[2,3], Kerkabou Abdeldjalil[1], Harsa Bouchra[4], Mekkiou Ratiba[1,*] Diana C.G.A. Pinto[5], and Artur M.S. Silva[5]

[1]*Unité de recherche: Valorisation des Ressources Naturelles, Molecules Bioactives et Analyses Physico-chimiques et Biologiques (VARENBIOMOL), Université Constantine 1 des Frères Mentouri*

[2]*Research Unit of Environmental Chemistry and Molecular Structural (CHEMS), University of Constantine1 des frères Mentouri, Constantine, Algeria*

[3]*Departmentof Process Engineering, Facultyof Process Engineering, University of Salah Boubnider Constantine 3, Constantine, Algeria*

[4]*University of Badji Mokhtar-Annaba, Faculty of Sciences, Department of Biology, Option of Vegetal Biology and Pharmacognosy, Laboratory of Plant Biology and Environment (LBVE), Axis: Medicinal Plants and Natural Substances, Bp 12, 23000 Annaba, Algeria*

[5]*LAQV-REQUIMTE & Department of Chemistry, University of Aveiro, 3810-193 Aveiro, Portugal*

Corresponding author: mekkiou_ratiba@yahoo.fr; mekkiou_ratiba@umc.edu.dz

Volume 7, Issue 8, Aug 2025
Received: 8th April, 2025
Accepted: 20th May, 2025
Published:01Aug2025
doi:10.48047/AFJBS.7.8.2025.190-204

Abstract

This study focuses on the plant *Suaeda fruticosa* Forssk. Ex J.F.Gmel, (Chenopodiaceae family), which is a halophyte species growing in salt lakes or Sebkha and belonging to the Saharan flora of Algeria. The GC/MS method was used to screen phytoconstituents of petroleum ether (PESF) extract from *S. fruticosa* aerial parts. An *in silico* molecular docking was conducted through two identified compounds of PESF extract. The GC/MS analysis permitted the identification of 32 compounds from which 1-octacosanol (37.23%), triacontanol (15.53%), followed by their relative aldehydes octacosanal (8.86%), triacontanal (7.49 %). DFT calculations and molecular docking simulations were conducted on the two selected compounds, Octacosanal and β-sitosterol, against the Acetylcholinesterase (AChE) enzyme (PDB ID: 6TT0) to compare their chemical reactivity, assess their structural properties, and evaluate their potential as anti-Alzheimer's agents. Our obtained finding demonstrated very high binding affinities with the enzyme, with values of -13.15 kcal/mol for Octacosanal and -10.26 kcal/mol for β-sitosterol.

Keywords: *Suaeda fruticosa*; GC/MS; Phytoconstituents; Anti-Alzheimer; DFT; Molecular docking; Octacosanal.

Introduction

Halophytes are interesting and particular plants that can grow and survive in high salinity conditions, they have developed unique physiological, biochemical and morphological mechanisms to tolerate and adapt to salt stress, including synthesizing bioactive secondary metabolites [1]. Halophytes are considered vegetables due to their organoleptic properties and salty taste, and medicinal plants due to the presence of bioactive compounds [2]. Natural products represent important reservoirs for both synthetic and traditional herbal medicines. Alzheimer's disease constitutes a domain in which natural products have not been fully utilized to their potential. Several researchers are carrying out preclinical trials using isolated bioactive compounds, and Ginkgo biloba (a plant extract) on Alzheimer's disease [3].

Numerous species of the *Suaeda* genus (Chenopodiaceae family), can be considered as substitute sources of high-quality edible oil in the region around the Mediterranean and Europe [4]. It is also frequently utilized as animal feed or green food in the regions where it grows [5].

Suaeda fruticosa (L.) Forsk. var. *longifolia* (Koch) Fenzl., called "Souida" in Arabic, "Soude buissonnante" in French, and "Sea-Blite" in English, is a halophyte plant that thrives in saline environments (Sebkha) in the Algerian Sahara [6]. It plays a crucial role in saline ecosystems and helps in stabilizing soil and preventing erosion [7]. The plant's ability to thrive in high salinity conditions makes it an excellent candidate for the restoration of salt-affected landscapes [8]. This species has been traditionally used for its medicinal properties [9-11].

According to the literature review conducted on the species *Suaeda fruticosa*, numerous studies have examined the chemical composition and diverse biological activities of polar extracts [9, 12-15]. For these reasons, and in continuation of our studies on Algerian species [16-22], this work aimed to investigate the chemical composition of lipophic fraction, Petroleum ether extract using GC/MS analysis, in addition, DFT calculations and molecular docking simulations were performed to analyze and compare the chemical reactivity of the two selected compounds and identify their binding affinity against the Acetylcholinesterase (AChE) enzyme (PDB ID: 6TT0). These analyses were conducted to assess the compounds structural properties and their potential as anti-Alzheimer's agents, evaluating their biological significance.

2. Material and Methods

2.1. Plant Material

Aerial parts of *Suaeda fruticosa* were collected from Ouargla region on Marsh 2021 and authentified by Dr. Bouchra Harsa (University of Annaba, Algeria). A voucher specimen was deposited in the herbarium of the VARENBIOMOL unit research of Mentouri brothers University of Constantine 1, Algeria; under the reference number CSF 3/21.

2.2. Extracts preparation

The aerial parts of *S. fruticosa* were dried at room temperature, then grounded into powder and subjected to a sequential extraction using solvents with increasing polarities. A quantity of 600 grams of powder was initially macerated in petroleum ether at room temperature for 45 minutes

three times. The resulting filtrates were then removed and the remaining powder was sequentially extracted with chloroform for 45 minutes three times then filtered. Each filtrate was concentrated at 30°C using a rotary evaporator and stored at 4° C until future use. Two different extracts were obtained: Petroleum ether extract (1g of PE), and chloroform extract (2.5g of CH). Both extracts were stored at 4° C until future use.

2.3. Silylation process

A quantity of 5.0 mg of PESF obtained from the aerial parts of *S. fruticosa* was accurately weighed into a 1 mL vial, then 15 µL of TMS (trimethylsilyl), 70 µL of pyridine, 65 µL of BSTFA (N,O-bis (triméthylsilyl) trifluoroacétamide), and 300 µL of eicosane used as internal standard (IS), were added. Subsequently, the vial was tightly capped and heated at 70°C for20 minutes, and 0.5 µL of the mixture was injected into the GC-MS apparatus.

2.4.GC-MS characterization of PE extract

The lipophilic composition of PE extract was analyzed on a Shimadzu Gas Chromatograph QP2010 Ultra coupled to the selective mass detector (Agilent 5975) equipped with an Autosampler AOC-20i. Separation was carried out using a capillary column DB-5 J & W capillary column (30 m × 0.25 mm inner diameter, 0.25 µm film thicknesses). At a flow rate of 35 cm/s, Helium was used as a gas. The identification of the compounds was performed from the interpretation of the fragmentation patterns and the comparison of the mass spectra obtained with data from the Wiley and NIST libraries and data previously reported in the literature.

2.5. DFT Calculations and Molecular docking

Initially, the geometries of the selected molecules were optimized using the ORCA program package at the B3LYP-D3/def2-TZVPP level of theory [23]. The chemical reactivity Descriptors of the two selected compounds, Octacosanal and β-sitosterol, were then calculated and compared with values reported in the literature [24-28]. Next, molecular docking studies were performed with the Auto Gridand AutoDock executable programs available in MGLtools (AutoDock Tools) [29]. Finally, the 3D crystal structure of the AChE enzyme (PDB ID: 6TT0) was retrieved from the Protein Data Bank (https://www.rcsb.org/structure/6TT0) [30].

For receptor preparation, all ligands (N9T and NAG), ions, and water molecules were removed. Non-polar hydrogens were then merged, and Kollman partial charges were added. Docking studies were carried out using the Lamarckian genetic algorithm (LGA). A 3D grid with dimensions of 80×80×80 points and a spacing of 0.375 Å was used. Among all docked poses, only the best one (i.e., the pose with the lowest binding energy) was selected, provided that its root-mean-square deviation (RMSD) was less than 1 Å. An exception was made for Octacosanal, where the RMSD exceeded 3 Å due to the molecule's elongated structure, making a smaller RMSD practically impossible. The best protein–ligand poses were visualized using Chimera (version 1.10.2) [31] and Discovery Studio Visualizer BIOVIA (version 20.1) [32].

3. Results and Discussion

3.1. GC/MS analysis

After a silylation reaction performed on 5mg of the PE extract of the aerial parts of *S. fruticosa* collected from the Ouargla region, Algeria, the GC-MS analysis permitted the identification of 32 compounds, representing 96.27 % of the total peaks, by comparing their mass spectra with NIST and Wiley libraries mass spectra. The identified compounds with their retention time and percentage area are summarized in Table 1.

The main constituents are long-chain fatty alcohols with an important percentage such as 1-octacosanol (37.23%), triacontanol (15.53%), followed by their relative aldehydes octacosanal (8.86%), triacontanal (7.49 %), moreover a group of 5 long-chain alkanes represents 4.55%, a group of 9 fatty acids represents 7.06%, and 15.55% of the rest of components.

Table 1. Components of the petroleum ether extract from *S. fruticosa*

Peak number	RT	Area%	Formula	name
1	6.596	0.15	$C_5H_{10}O_3$	3-hydroxyisovaleric acid
2	9.748	0.21	$C_{10}H_8N_2$	2,2'-bipyridine
3	10.613	0.05	$C_{11}H_{16}O_2$	2(4H)-benzofuranone,5,6,7,7a-tetrahydro-4,4,7a-trimethyl-,(R)-
4	13.241	0.11	$C_{19}H_{38}OSi$	1-(t-butyldimethylsilyl)-4-(2,2-dimethyl-6-methylene-cyclohexyl)-butan-1-ol
5	13.877	0.18	$C_{18}H_{36}O$	2-Pentadecanone,6,10,14-trimethyl
6	15.948	9.39	$C_{20}H_{42}$	Eicosane
7	16.491	0.69	$C_{16}H_{32}O_2$	Palmitic acid
8	18.727	0.09	$C_{18}H32O_2$	Linoleic acid
9	18.812	0.16	$C_{18}H_{34}O_2$	Oleic acid
10	19.176	0.18	$C_{18}H_{36}O_2$	Stearic acid
11	20.793	0.69	$C_{18}H_{35}NO$	9-octadecenamide,(z)-
12	21.82	0.07	$C_{20}H_{40}O_2$	Arachidic acid
13	22.692	0.07	$C_{19}H_{40}$	Nonadecane
14	24.728	0.14	$C_{22}H_{44}O_2$	Behenic acid
15	25.745	0.57	$C_{21}H_{44}$	Heneicosane
16	28.059	0.77	$C_{26}H_{52}O$	Hexacosanal
17	29.148	1.44	$C_{28}H_{58}$	Octacosane
18	29.152	2.17	$C_{29}H_{60}$	n-nonacosane
19	29.878	1.17	$C_{25}H_{50}O_2$	Pentacosanoic acid
20	31.717	8.86	$C_{28}H_{56}O_2$	Octacosanal
21	32.731	0.3	$C_{25}H_{52}$	2-methyl tetracosane
22	33.547	37.23	$C_{28}H_{58}O$	1-octacosanol
23	35.186	1.88	$C_{28}H_{56}O_2$	octacosanoate
24	35.45	7.49	$C_{30}H_{60}O$	Triacontanal
25	36.647	0.73	$C_{29}H_{50}O$	beta-sitosterol
26	36.868	0.37	$C_{29}H_{52}O$	stigmastanol
27	37.153	15.53	$C_{30}H_{62}O$	Triacontanol
28	38.825	2.68	$C_{30}H_{60}O_2$	triacontanoate
29	39.158	0.98	$C_{32}H_{64}O$	dotriacontanal
30	39.598	0.46	$C_{57}H_{104}O_6$	9-octadecenoic acid 1,2,3-propanetriyl ester
31	39.706	0.66	$C_{39}H_{72}O_5$	Di-(9-octadecenoyl)-Glycerol
32	41.015	0.8	$C_{35}H_{74}OSI$	silane,(dotriacontyloxy)trimethyl

In previous studies, it was mentioned that lipid extract of some halophytes species contains fatty alcohols as main components [33-34], and the length of their chains vary from species to another. However, the amount of the bioactive compound octacosanol (37.26%) [35] seems important especially that we have again 8.86% of the octacosanal which could be an intermediate in octacosanol biosynthesis [36].

Octacosanol which is the main constituent in *Suaeda fruticosa* petroleum ether extract exhibits multiple biological activities. It can inhibit TNF-α production and reduces leukocyte influx in

inflammatory models, reduces hepatic lipid accumulation, suppresses MAPK/NF-κB signaling pathways, and lowering inflammation in liver tissues [37-38]. Besides, Octacosanol enhances gluthatione levels, scavenging reactive oxygen species and mitigating oxidative stress [39]. Finally, a recent study on hexane extract of the same species has shown that it is an anti-cancer agent [40].

3.2. DFT calculations

It has been reported in the literature that the stability of a molecule is associated with the energy gap (ΔE_{gap}) between the HOMO and LUMO, where a larger gap indicates higher stability, while a smaller gap corresponds to increased reactivity [41-42].

The energy gap results, presented in Table 2, show that Octacosanal has the lowest energy gap and the highest softness (i.e., the lowest hardness), suggesting greater chemical reactivity compared to β-sitosterol. However, both molecules exhibit comparable values of total energy (Octacosanal: -1163.378 Eh, β-sitosterol: -1210.044 Eh) and dipole moments (Octacosanal: 1.515 Debye, β-sitosterol: 1.567 Debye).

Table 2 The calculated quantum chemical descriptors[(a)] of the two selected compounds.

	Octacosanal	**β-sitosterol**
$\mathbf{E_{HOMO}}$	-5.351	-6.355
$\mathbf{E_{LUMO}}$	-1.913	0.422
$\mathbf{\Delta E_{gap}}$	3.438	6.777
μ (Debye)	1.515	1.567
Total Energy (Eh)	-1163.378	-1210.044
χ	3.632	2.966
η	1.719	3.388
σ	0.582	0.295
ω	3.837	1.298

[(a)]: $\mathbf{E_{HOMO}}$: Energies of highest occupied molecular orbital, $\mathbf{E_{LUMO}}$: Energies of lowest unoccupied molecular orbital, $\mathbf{\Delta E_{gap}}$: Energy gap. **μ**: Dipole moment, **χ**: Electronegativity, **η**: Global hardness, **σ**: Global softness, and **ω**: Global electrophilicity.

Frontier molecular orbitals (FMOs), specifically the highest occupied molecular orbital (HOMO) and the lowest unoccupied molecular orbital (LUMO), are commonly used in reactivity studies to identify and analyze the most reactive sites, serving as reactive centers for both electrophilic and nucleophilic attacks [41-42].

The optimized molecular structures of Octacosanal and β-sitosterol, along with their FMO density distributions (HOMO and LUMO), are presented in Fig. 1.

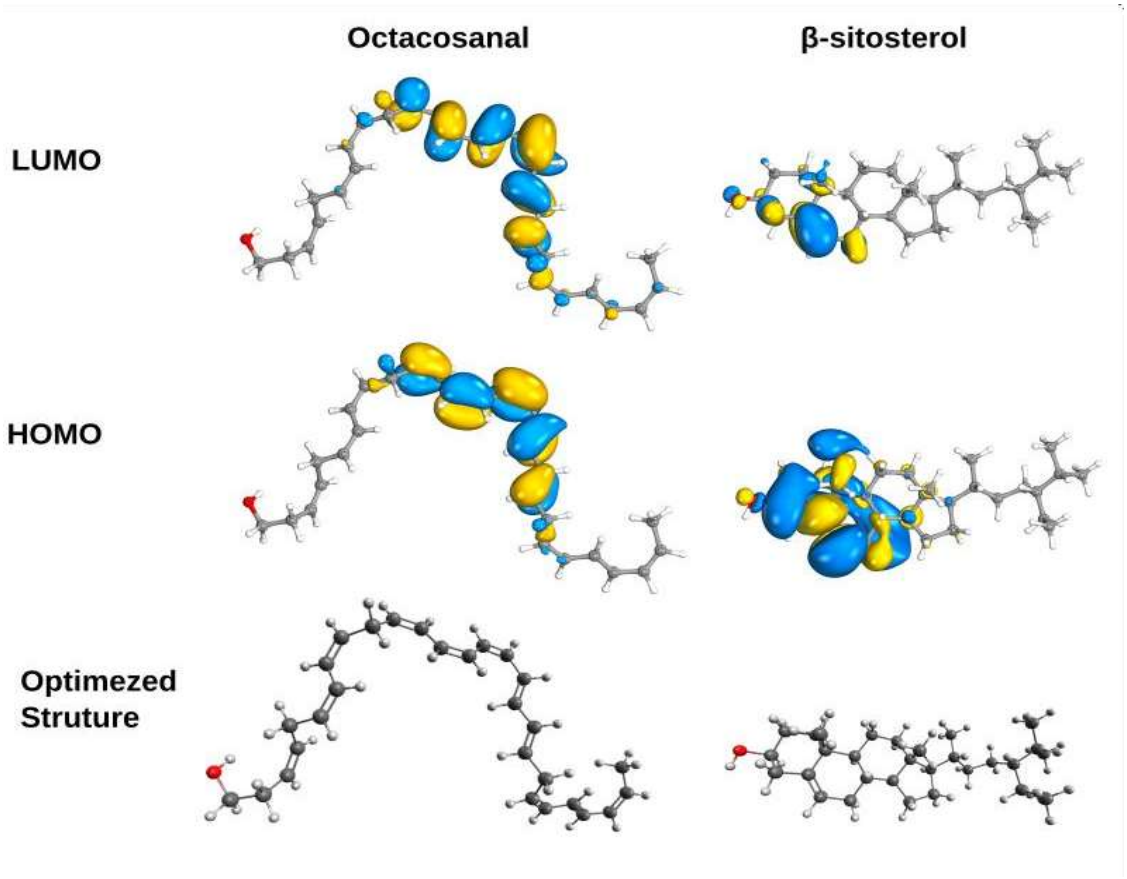

Fig. 1. Optimized structures and the frontier molecular orbitals (HOMO and LUMO) of Octacosanal and β-sitosterol molecules.

The analysis of the FMO density distributions (see Fig. 1) reveals that, in the case of the Octacosanal molecule, the HOMO and LUMO orbitals are predominantly localized in the middle of the chain at the twenty-eighth carbon, due to the resonance of the -C=C-C=C- system. On the other hand, for the β-sitosterol molecule, the HOMO and LUMO densities are concentrated on the hydroxyl group and the two rings at the end of the phenanthrene framework. This indicates that the most reactive centers of the selected compounds can preferentially interact with other chemical species by donating and/or accepting electrons.

3.3. Molecular docking

Table 3 presents the docking analysis findings, detailing key interaction parameters between the selected molecules (Octacosanal and β-sitosterol) and the binding sites of the AChE enzyme (PDB ID: 6TT0). The reported values include predicted free binding energy (BE), estimated inhibition constant (KiC), total intermolecular energy (TIE), final total internal energy (FIE), and electrostatic energy (EE), corresponding to the most favorable docking poses.

According to the docking results (Table 3), Octacosanal and β-sitosterol exhibit strong binding affinities toward the 6TT0 target, with binding free energies of -13.15 kcal / mol and -10.26 kcal/mol, respectively. This difference is also evident in the inhibition constants (Ki), with Octacosanal exhibiting a value of 229.93 pM, suggesting stronger inhibitory potential than β-

sitosterol, which has a Ki of 30.37 nM. It is worth highlighting that Octacosanal and β-sitosterol demonstrate stronger binding affinities compared to the reference ligand N9T ((1R, 3S)-3-(benzylamino)-N-(6,7-dimethoxy-2-oxochromen-3-yl)cyclohexane1carboxamide), which binds to the 6TT0 receptor with a free energy of -11.22 kcal/mol.

The contributions of van Der Waals interactions, hydrogen bonds, and desolvation are slightly more favorable for Octacosanal (-15.25 kcal/mol) than for β-sitosterol (-14.94 kcal/mol).

Table 3. Calculated parameters (a–h) for the candidate ligands Octacosanal and β-sitosterol at the Acetylcholinesterase (AChE) enzyme (PDB ID: 6TT0).

	Octacosanal	**β-sitosterol**
BE [(a)]	-13.15	-10.26
KiC [(b)]	229.93 pM	30.37 nM
FIE [(c)]	-15.24	-15.03
WHD [(d)]	-15.25	-14.94
EE [(e)]	+0.01	-0.09
TIE [(f)]	-0.82	-2.09
Torsional Free Energy [(g)]	+2.09	+4.77
RMSD [(h)]	0.857	3.422

[a] **BE**: Free Energy of Binding (kcal/Mol).
[b]**KiC**; Estimated Inhibition Constant, Ki. (pM: picomolar & nM: nanoMolar);
[c] **FIE** : Final Intermolecular Energy;
[d]**WHD**: vdW + Hbond + desolv Energy ;
[e] **EE**: Electrostatic Energy (kcal/Mol)
[f] **FTIE**: Final Total Internal Energy;
[g] **TFE**: Torsional Free Energy (kcal/Mol);
[h] **RMSD**: Root Main square Diviation.

In terms of electrostatic energy, Octacosanal shows a marginally positive value (+0.01 kcal/mol), whereas β-sitosterol presents a slight negative value (-0.09 kcal/mol), highlighting differences in the electrostatic interactions of the two compounds. Octacosanal also demonstrates a more favorable total internal energy (-0.82 kcal/mol) and a less restrictive torsional free energy (+2.09 kcal/mol) compared to β-sitosterol. These findings suggest that Octacosanal exhibits a stronger affinity for the target, as illustrated in Table 3.

The 2D and 3D visualizations of the β-sitosterol@6TT0 and Octacosanal@6TT0 complexes, highlighting the best binding poses and the interacting amino acid residues, are shown in Fig. 2 and 3, respectively. Table 4 provides a detailed list of the interacting amino acids along with their corresponding distances (Å).

Table 4. The amino acids involved in interactions of Octacosanal, β-sitosterol ligands at the Acetylcholinesterase (AChE) enzyme (PDB ID: 6TT0).

Comp.	*Amino acid involved in interaction (Interaction site)*	**Distances (Å)**
Octacosanal@6TT0	Arg289, Ser286, Ile287,Phe290, Tyr121, Tyr334, Phe331, Trp84, Phe330, His440.	Lig−Arg289, (1.99) Lig−Phe330, (3.87) Lig−Ser286, (3.44) Lig−Ile287, (5.27) Lig−Phe290, (4.84) Lig−Tyr121, (5.48) Lig−Tyr334, (4.57) Lig−Phe331, (4.44; 5.46) Lig−Trp84, (5.30; 5.35; 4.88; 5.23) Lig−Phe330, (3.87) Lig−His440, (4.39; 5.46)
β-sitosterol @6TT0	Phe330, Phe331, Tty334, Tyr121, Trp279, Ile287 & Tyr70.	Lig−Phe330, (3.37) Lig−Phe331, (4.36; 5.22) Lig−Tyr334, (3.87; 4.22) Lig−Tyr121, (5.44) Lig−Trp279, (4.33; 4.37) Lig−Ile287, (5.32; 5.43) Lig−Tyr70, (5.09)

The Octacosanal ligand interacts with the 6TT0 binding site through a conventional hydrogen bond between the hydrogen atom of its hydroxyl group and the oxygen atom of the carbonyl function of the Arg289 residue (1.99 Å), as well as a carbon-hydrogen bond with Ser286(3.44Å). These interactions are illustrated in Figure 2 (band c) and detailed in Table 4.

On the other hand, hydrophobic interactions, particularly alkyl and π-alkyl interactions play a crucial role in stabilizing the Octacosanal@6TT0 complex (Fig. 2 c). These interactions involve several amino acid residues, including Ile287 (5.27 Å), Phe290 (4.84 Å), Tyr121 (5.48 Å), Tyr334 (4.57 Å), Phe331 (4.44 Å; 5.46 Å), Trp84 (5.30Å; 5.35 Å; 4.88Å; 5.23 Å), Phe330 (3.87Å), and His440 (4.39 Å; 5.46 Å).

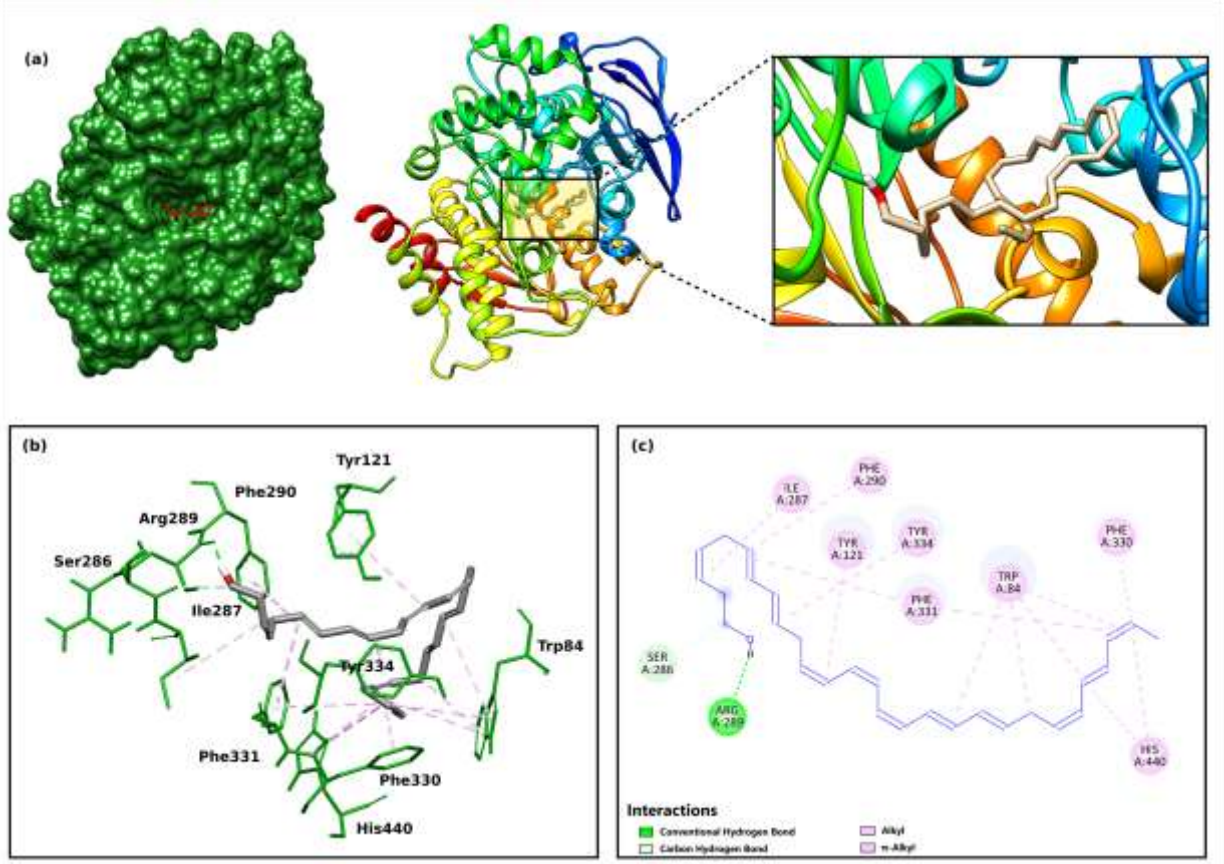

Fig. 2. 2D and 3D representations of the optimal binding pose of the Octacosanal@6TT0 complex.

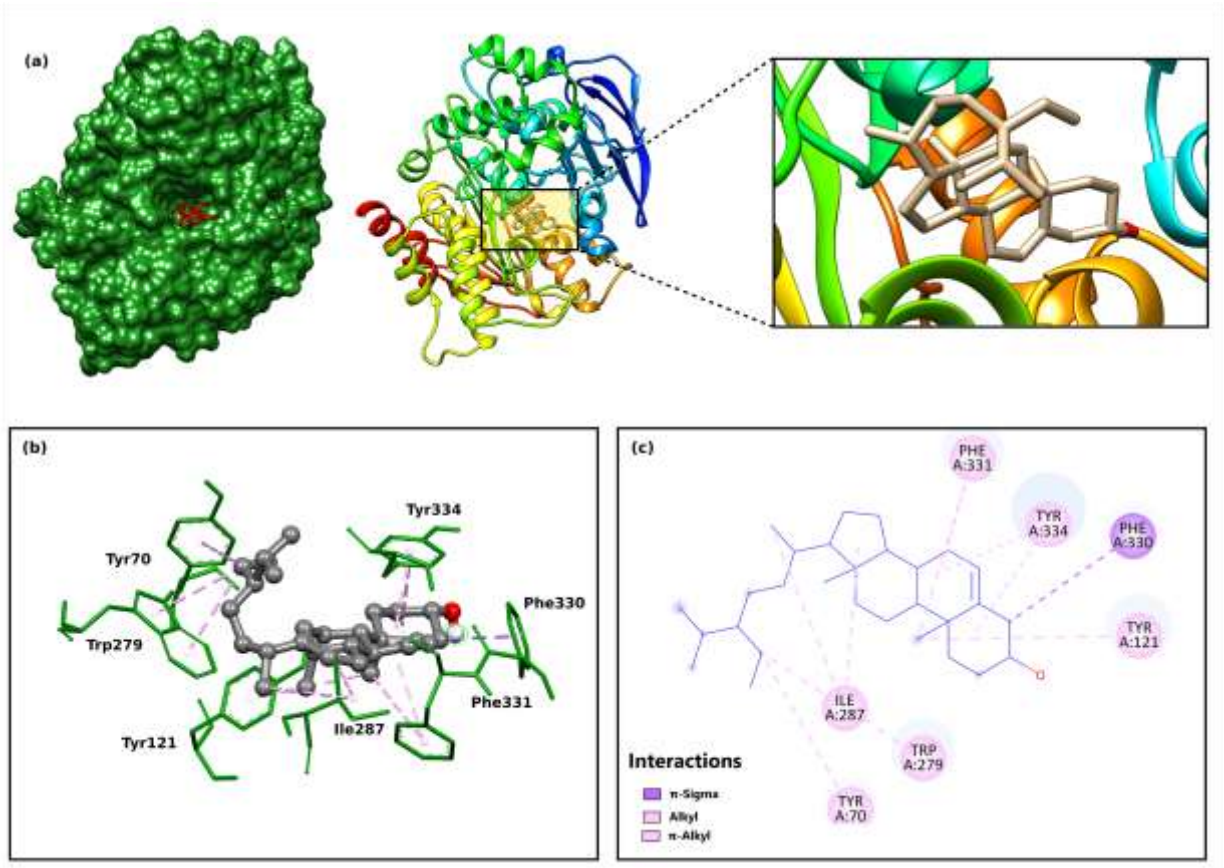

Fig. 3. 2D and 3D representations of the optimal binding pose of the β-sitosterol@6TT0 complex.

The docking analysis reveals that β-sitosterol interacts with the 6TT0 target through multiple stabilizing interactions involving key amino acid residues. Notably, a π-sigma interaction is observed with Phe330 (3.37 Å), while a combination of π-sigma and π-alkyl interactions is established with several residues, including Phe331 (4.36 Å; 5.22 Å), Tyr334 (3.87Å; 4.22Å), Tyr121(5.44Å),Trp279 (4.33Å;4.37Å), Ile287 (5.32Å;5.43Å), and Tyr70 (5.09 Å). These interactions highlight the significant role of hydrophobic forces in stabilizing the β-sitosterol@6TT0 complex, contributing to its strong binding affinity with the target (see Table 4 and Fig. 3).

Conclusion

In the present research, the chemical investigation of *Suaeda fruticosa* Petroleum ether extract was analyzed using the GC/MS technique. The results revealed that this lipophilic extract is rich in saturated primary fatty alcohols, where 1- octacosanol (37.23%), and triacontanol (15.53%), are the major compounds followed by their relative aldehydes octacosanal (8.86%), triacontanal (7.49 %), and a group of 9 fatty acids represents 7.06%. DFT approaches and molecular docking study were performed to analyze and compare the chemical reactivity of the major constituents and identify their binding affinity against the Acetylcholinesterase (AChE) enzyme (PDB ID: 6TT0). Octacosanal and β-sitosterol exhibit strong binding affinities toward the 6TT0 target, with free energies of -13.15 and -10.26 kcal/mol, respectively, surpassing the binding affinity of the reference ligand N9T. Therefore, the lipophilic extract of *S. fruticosa* would be a promising alternative which must be supported by additional investigations as well as pharmacodynamic and pharmacokinetic studies.

Conflict of Interest

The authors declare no conflict of interest.

Authors' Declaration

The authors hereby declare that the work presented in this article is original and that any liability for claims relating to the content of this article will be borne by them.

Acknowledgments

The authors thank the DGRSDT-Algeria for providing a research grant (PRFU Project B00L01UN250120220011).

References

1. Mann, A.; Lata, C.; Kumar, N.; Kumar, A.; Kumar, A.; Sheoran, P. Halophytes as new model plant species for salt tolerance strategies. *Front. Plant Sci.* **2023**, *14*, 1137211. doi: 10.1016/ j.dib.2021.107536.
2. Maatallah Zaier M., Ciudad-Mulero M.; Cámara, M.; Pereira, C.; Ferreira, I.C.F.R.; Achour, L.; Kacem, A.; Morales, P. Revalorization of Tunisian wild Amaranthaceae halophytes: Nutritional composition variation at two different phenotypes stages. J. Food Compos. Anal. **2020**, 89, 103463.
3. Xin Chen, Joshua Drew, Wren Berney, Wei Lei. Neuroprotective Natural Products for Alzheimer's Disease. Cells, 2021 May 25;10(6):1309. doi: 10.3390/cells10061309
4. García-Rodríguez, A., & González-Muñoz, M. (2019). *The potential of halophytes from the Suaeda genus as sources of edible oils for the Mediterranean region. Environmental and Experimental Botany*, 161, 229-238. https://doi.org/10.1016/j.envexpbot.2019.03.003.
5. Abideen, Z., & Bhatti, H. N. (2013). *The potential of halophytes as livestock fodder and green food in saline environments. Acta Botanica Croatica*, 72(1), 71-79. https://doi.org/10.2478/botcro-2013-0009.
6. Zid, E. H., & Foudhaily, M. (2017). *Ecology and ethnobotany of Suaeda fruticosa (L.) Forsk. var. longifolia (Koch) Fenzl. in the Algerian Sahara: A halophyte of great potential. Acta Botanica Gallica*, 164(3), 347-355. https://doi.org/10.1080/12538078.2017.1305878.
7. Devi S., Nandwal A.S., Angrish R., Arya S.S., Kumar N. & Sharma S.K.. Phytoremediation potential of some halophytic species for soil salinity. *International Journal of Phytoremediation.* 2016, VOL. 18, NO. 7, 693–696 doi.org/10.1080/15226514.2015.1131229.
8. Ungar, I. A. (1991). *Ecology of salt-affected soils and vegetation.* In J. B. Grace & D. L. Tilman (Eds.), *Perspectives on plant competition* (pp. 211-227). Academic Press.
9. Oueslati, S.; Ksouri, R.; Falleh, H.; Pichette, A.; Abdelly, C.; Legault, J. Phenolic content, antioxidant, anti-inflammatory and anticancer activities of the edible halophyte *Suaeda fruticosa* Forssk. *Food Chem.* **2012**, *132*, 943–947.
10. Ullah, S.; Bano, A.; Girmay, S.; Tan, G. Anticancer, antioxidant and antimicrobial activities of *Suaeda fruticosa* related to its phytochemical screening. *Int. J. Phytoremed.* **2012**, *4*, 284.
11. Ahmad, I.; Gul, H.; Noureen, A.; Ujjan, J.A.; Manzoor, S.; Muhammad, W. Antimicrobial, Antioxidant and Antidiabetic Potential of *Suaeda fruticosa* L. *Int. J. Emerg. Technol.* **2021**, *12*, 155–160.
12. Afsheen Ayaz, QurratUlAin Jamil, Musaddique Hussain, Fayyaz Anjum, Adeel Sarfraz, Taha Alqahtani, Nadia Hussain, Reem M. Gahtani, Ayed A. Dera, Hanan M. Alharbi and Shahid M. Iqbal. Antioxidant and Gastroprotective Activity of *Suaeda fruticosa* Forssk. Ex J.F.Gmel. *Molecules* **2022**, *27*(14), 4368; **Doi.org/10.3390/molecules27144368**.
13. Muhammad Fiaz, Mohamed Farouk Elsadek, Khalid S. Al-Numair, Shafqat Rasul Chaudhry, Mohammad Saleem, Kashif ur Rehman Khan, Ashwaq Hamid Salem Yehya & Muhammad Asif. Down-regulationof interlinked inflammatory signalling cascades by ethanolic extract of Suaeda fruticosa Forssk. Ex J.F. Gmel. Attenuated in vivo inflammatory and nociceptive responses. Inflammopharmacology, 2025, Vol 33; 311-328.
14. Hammad Saleem, Umair Khurshid, Muhammad Sarfraz, Muhammad Imran Tousif, Abdulwahab Alamri, Sirajudheen Anwar, Abdulhakeem Alamri, Irshad Ahmad, Hassan H. Abdallah, Fawzi M. Mahomoodally, Nafees Ahemad. A comprehensive phytochemical,

biological, toxicological and molecular docking evaluation of *Suaeda fruticosa* (L.) Forssk.: An edible halophyte medicinal plant. Food and Chemical Toxicology; 2021, Volume 154, 112348. https://doi.org/10.1016/j.fct.2021.112348.

15. Maatallah Zaier M., Heleno S. A., Mandim F., Calhelha R. C., Ferreira I. C.F.R., Achour L., Kacem A., Dias M. I., Barros L. Effects of the seasonal variation in the phytochemical composition and bioactivities of the wild halophyte *Suaeda fruticosa.* Food Bioscience; Volume 50, Part B, 2022, 102131. Doi.org/10.1016/j.fbio.2022.102131.
16. Azzouzi M., Mekkiou R., Chalard P., Chalchat J.C., Boumaza O., Seghiri R., Benayache F. and Benayache S. (2016). Essential Oil Composition of CentaureachoulettianaPomel (Asteraceae) from Algeria, *International Journal of Pharmacognosy and PhytochemicalResearch*, **8**(9), 1545–1548.
17. Sara Zerrouki, Samia Mezhoud, Mustafa Abdullah Yilmaz, Ayse Sahin Yaglioglu, Derya Bakir, Ibrahim Demirtas & Ratiba Mekkiou. LC/MS-MS Analyses and *in vitro* anticancer activity of *Tourneuxia variifolia* extracts. Natural Product Research, 2021. 36(17). 4500-4504. DOI: 10.1080/14786419.2021.1986818.
18. Sara Zerrouki**,** Samia Mezhoud, Ayse Sahin Yağlioğlu, Chawki Bensouici, Mehmet Nuri Atalar, Ibrahim Demirtas, Souad Ameddah and Ratiba Mekkiou. Antioxidant, anticancer activities, and HPLC-DAD analyses of the medicinal halophyte *Limoniastrum guyonianum* Dur. Extracts. J.Res. Phar.2022. 26. 598-608.
19. Manel Boumaraf, Abdeldjalil Kerkabou, Nabila Slougui, Djamel Sarri, Chawki Bensouici, Hazmoune Hichem and Ratiba Mekkiou. *In-vitro* assessment of α-amylase, photoprotective, antimicrobial activities, and chemical composition of *Asphodelus microcarpus* (Liliaceae) essential oils from constantine. Global NEST Journal, 2024; Vol 26, No 8, 05854. doi.org/10.30955/gnj.05854.
20. Boussaha S., Bramucci M., Rebbas K., Quassinti L., Mekkiou R., Maggi F. Chemical composition and anticancer activity of the essential oil from *Vicia ochroleuca* Ten., quite rare plant in Kabylia (Algeria). Nat. Prod. Res. 2023, 37, 1–7. Doi.org/10.1080/14786419.2023.2176492.
21. Samia Mezhoud, Sara Zerrouki, Hanane Aissaoui, Jean-Claude Chalchat, Pierre Chalard, Fadila Benayache, Samir Benayache and Ratiba Mekkiou. GC/MS analysis of the essential oil composition of *Tourneuxia variifolia* Coss. growing in the Algerian Sahara. *Afr.J.Bio.Sc. 6(13) (2024). Doi.org/10.48047/AFJBS.6.13.2024.5087-5096.*
22. Bouchra Harsa, Ratiba Seridi, Ratiba Mekkiou, Abdeldjalil Kerkabou, Nina Sadou, Chawki Bensouici and Amina Chouh. Phytochemical screening and biological activities of *Pallenis hierochuntica* extracts during fructification in the Betita region, Algeria. *Afr.J.Bio.Sc. 6(14) (2024). Doi.org/10.48047/AFJBS.6.14.2024.10046-10059.*
23. F. Weigend, R. Ahlrichs, Balancedbasis sets of split valence, triplezeta valence and quadruplezeta valence quality for H to Rn: Design and assessment of accuracy, Phys. Chem. Chem. Phys. 7 (2005) 3297. https://doi.org/10.1039/b508541a.
24. N. Ammouchi, H. Allal, E. Zouaoui, K. Dob, D. Zouied, M. Bououdina, Extracts of Ruta Chalepensis as Green Corrosion Inhibitor for Copper CDA 110 in 3% NaCl Medium: Experimental and Theoretical Studies, 11 (2019).
25. H. Allal, H. Nemdili, M.A. Zerizer, B. Zouchoune, Molecular structures, chemical descriptors, and pancreatic lipase (1LPB) inhibition by natural products: a DFT investigation

and molecular docking prediction, Struct Chem 35 (2024) 223–239. https://doi.org/10.1007/s11224-023-02176-2.

26. J. S.Al-Otaibi, Y.S. Mary, Y.S. Mary, S.J. Armaković, S. Armaković, C. Van Alsenoy, H.S. Yathirajan, Insights into the reactivity properties, docking, DFT and MD simulations of orphenadrinium dihydrogen citrate in different solvents, J Mol Liq 367 (2022) 120583. https://doi.org/10.1016/j.molliq.2022.120583.
27. R. Khelifi, N. Latelli, Z. Charifi, H. Baaziz, H. Chermette, Predicting the activity of methoxyphenol derivatives antioxidants: I. Structure and reactivity of methoxyphenol derivatives, a DFT approach, Comput Theor Chem 1229 (2023) 114287. https://doi.org/10.1016/j.comptc.2023.114287.
28. M. Taier, H. Allal, S. Bousba, F. Bouhadiouche, S. Maza, M. Damous, A. Boussadia, A computational investigation on the adsorption behavior of bromoacetone on B36 borophene nanosheets, J Comput Electron 23 (2024) 931–944. Doi.org/10.1007/s10825-024-02192-3.
29. J.P. Arcon, C.P. Modenutti, D. Avendaño, E.D. Lopez, L.A. Defelipe, F.A. Ambrosio, A.G. Turjanski, S. Forli, M.A. Marti, AutoDock Bias: improving binding mode prediction and virtual screening using known protein–ligandinteractions, Bioinformatics 35(2019)3836–3838. Doi.org/10.1093/bioinformatics/btz152.
30. M. Catto, L. Pisani, E. De La Mora, B.D. Belviso, G.F. Mangiatordi, A. Pinto, A. De Palma, N. Denora, R. Caliandro, J.-P. Colletier, I. Silman, O. Nicolotti, C.D. Altomare, Chiral Separation, X-ray Structure, and Biological Evaluation of a Potent and Reversible Dual Binding Site AChE Inhibitor, ACS Med. Chem. Lett. 11 (2020) 869–876. https://doi.org/10.1021/acsmedchemlett.9b00656.
31. E.F. Pettersen, T.D. Goddard, C.C. Huang, G.S. Couch, D.M. Greenblatt, E.C. Meng, T.E. Ferrin, UCSF Chimera—A visualization system for exploratoryresearch and analysis, J Comput Chem 25 (2004) 1605–1612. https://doi.org/10.1002/jcc.20084.
32. P.F. Ayodele, A. Bamigbade, O.O. Bamigbade, I.A. Adeniyi, E.S. Tachin, A.J. Seweje, S.T. Farohunbi, Illustrated Procedure to Perform Molecular Docking Using PyRx and Biovia Discovery Studio Visualizer: A Case Study of 10kt With Atropine, Prog Drug Discov Biomed Sci 6 (2023). https://doi.org/10.36877/pddbs.a0000424.
33. Isca, V.M.S., Seca, A.M.L., Pinto, D.C.G., Silva, H., Silva, A.M.S., Lipophilic profile of the edible halophyte *Salicornia ramosissima*. Food Chemistry, 2014. 05, 117. http://dx.doi.org/10.1016/j.foodchem.2014.05.117
34. H.M. Radwan, N.M. Nazif, L.M. Abou-Setta Phytochemical Investigation of Salicornia fruticosa (L.) And Their Biological Activity, Research Journal of Medicine and Medical Sciences, 2(2): 72-78, 2007.
35. Yaping Zhou, Fuliang Cao, Feijun Luo, Qinlu Lin, Octacosanol and health benefits: Biological functions and mechanisms of action, food biosciences 2022, 47, 101632 https://doi.org/10.1016/j.fbio.2022.101632.
36. Ying-Xiu Cao, Wen-Hai Xiao, Duo Liu, Jin-Lai Zhang, Ming-Zhu Ding, Ying-Jin Yuan, Biosynthesis of odd-chain fatty alcohols in *Escherichia coli*. Metabolic Engineering. 2015 May; 29:113-123. doi: 10.1016/j.ymben.2015.03.005.
37. Anderson Marques de Oliveira, Lucia M Conserva, Jamylle N de Souza Ferro, Fabíola de Almeida Brito, Rosângela P Lyra Lemos, Emiliano Barreto. Antinociceptive and Anti-Inflammatory Effects of Octacosanol from the Leaves of *Sabicea grisea* var. *grisea* in Mice. Int

J Mol Sci. 2012 Feb 2;13(2):1598–1611. doi: 10.3390/ijms13021598.

38. Jie Bai, Tao Yang, Yaping Zhou, Wei Xu, Shuai Han, Tianyi Guo, Lingfeng Zhu, Dandan Qin, Yi Luo, Zuomin Hu, Xiaoqi Wu, Feijun Luo, Bo Liu, Qinlu Lin. Octacosanol Modifies Obesity, Expression Profile and Inflammation Response of Hepatic Tissues in High-Fat Diet Mice. Foods. 2022 May 30;11(11):1606. doi: 10.3390/foods11111606.
39. Mahesh K. Kaushik, Kosuke Aritake, Atsuko Takeuchi, Masachi Yanagisawa and Yoshihiro Urade. Octacosanol restores stress-affected sleep in mice by alleviating stress. Scientific Reports | 7: 8892 | DOI:10.1038/s41598-017-08874-2.
40. Saleh KA, Albinhassan TH, Al-Ghazzawi AM, Mohaya A, Shati AA, Ayoub HJ, et al. Anticancer property of haexane extract of Suaeda fruticosa plant leaves against different cancer cell lines. Trop J Pharm Res. 2020, 19(1), 129-136. Doi: 10.4314/tjpr.v19i1.20
41. F. Bouhadouache, H. Allal, M. Taier, M. Damous, S. Maza, S. Bousba, A. Boussadia, E. Zouaoui, ADFT study of the adsorption of vanillin on Al(111) surfaces, Struct Chem 35 (2024) 1241–1253. https://doi.org/10.1007/s11224-023-02277-y.
42. M.S. Mohamad Sidik, M.H. Abu Bakar, H. Allal, Adsorption of Benzene-1,4-diol, 3-Methyl-1,2- cyclopentanedione and 2,6-Dimethoxyphenol on aluminium (1 1 1) plane using density functional theory calculations, Chemical Physics 560 (2022) 111592. https://doi.org/10.1016/j.chemphys.2022.111592.